

Received: 2017.04.04  
Accepted: 2017.04.18  
Published: 2017.05.28

# Zinc Finger E-Box Binding Protein 2 (ZEB2) Suppress Apoptosis of Vascular Endothelial Cells Induced by High Glucose Through Mitogen-Activated Protein Kinases (MAPK) Pathway Activation

Authors' Contribution:

Study Design A  
Data Collection B  
Statistical Analysis C  
Data Interpretation D  
Manuscript Preparation E  
Literature Search F  
Funds Collection G

ABC 1 **Lin-Jun Wang\***  
CD 2 **Zi-Heng Wu\***  
EF 3 **Xiang-Tao Zheng**  
DE 4 **Jian-Yun Long**  
EF 1 **Yang-Min Dong**  
AEFG 4 **Xin Fang**

1 Department of Vascular Surgery, Hangzhou Third Hospital, Hangzhou, Zhejiang, P.R. China  
2 Department of Vascular Surgery, The First Affiliated Hospital, School of Medicine, Zhejiang University, Hangzhou, Zhejiang, P.R. China  
3 Department of Vascular Surgery, The First Affiliated Hospital of Wenzhou Medical University, Wenzhou, Zhejiang, P.R. China  
4 Department of Vascular Surgery, Hangzhou First People's Hospital and Nanjing Medical University, Hangzhou Zhejiang, and Nanjing, Jiangsu, P.R. China

\* Lin-Jun Wang and Zi-Heng Wu contributed equally to the article

**Corresponding Author:** Xin Fang, e-mail: [fangxin7878@163.com](mailto:fangxin7878@163.com)

**Source of support:** This work was supported by National Natural Science Foundation of China (81200233), Natural Science Foundation of Zhejiang province of China (Grant No.LY16H020004/LY17H020011) and Zhejiang Medicine and Health Science and Technology Program (2014KYA080)

**Background:** Hyperglycemia has been confirmed to damage endothelial function of vascular and microvascular. The regulation of zinc finger E-box binding protein 2 (ZEB2) on vascular endothelial cells (VECs) is reported rarely. Our study investigates the role of ZEB2 on the apoptosis of VECs induced by high glucose through MAPK pathway.

**Material/Methods:** Downregulated and upregulated expression of ZEB2 in human umbilical vein endothelial cells (HUVECs) were performed by plasmids transfection. HUVECs are respectively treated with different concentrations of glucose (5.5 mM, 33 mM). The expression of mRNA and protein were detected by real-time quantified PCR and western blotting. Apoptotic cells were measured by flow cytometry. Proliferation and migration of HUVECs were detected by MTT assay and wound healing assay.





**Results:** The apoptosis of HUVECs detected by flow cytometry and western blot revealed that ZEB2 overexpression distinctly suppressed the apoptosis of HUVECs induced by high glucose. ZEB2 overexpression promoted the proliferative and migration activity of HUVECs. Besides, ZEB2 overexpression specifically accelerated the phosphorylation level of JNK, and suppressed the apoptosis and promoted the proliferative of VECs via JNK pathway.

**Conclusion:** ZEB2 suppress apoptosis of VECs induced by high glucose through MAPK pathway activation, which provides a novel insight and therapeutic target for endothelial injury.

**MeSH Keywords:** **Apoptosis • Endothelial Cells • Human Umbilical Vein Endothelial Cells • MAP Kinase Kinase Kinases • Zinc Fingers**

**Abbreviation:** **ZEB2** – zinc finger E-box binding protein 2; **VECs** – vascular endothelial cells; **HUVECs** – human umbilical vein endothelial cells

**Full-text PDF:** <http://www.medscimonit.com/abstract/index/idArt/904678>

 2550  —  5  26



## Background

*In vivo* and *in vitro*, studies have found that hyperglycemia could inhibit the growth of endothelial cells and induce apoptosis. Current researches have considered that vascular endothelial cells (VECs) injury and dysfunction are initial factors resulting in vascular complication induced by abnormal blood glucose [1]. Apoptotic mechanism of VEC has not been completely discovered. Probable pathogeny includes increasing of ROS, glycosylation end products (AGEs), activation of protein kinase C (PKC) and so on [2,3]. VECs could synthesis and secrete a variety of active factors, such as prostacyclin (PG), nitric oxide (NO) and endothelin-1 (ET-1), and participate in many physiological and pathological processes in body [4,5]. In diabetes status, eNOS decoupling significantly decreases the NO synthesis, however, it promotes reactive oxygen species (ROS) generation. The enhanced generation of ROS induced by oxidative stress is considered to be the critical factor of VECs apoptosis. High glucose could damage endothelial cell function through various mechanisms, such as inflammation, oxidative stress [6], secondary lipid metabolic disturbance [7], etc.

Zinc finger E-box binding protein (ZEB) is a kind of transcriptional regulators, which participate in regulation of VECs on the physiological or pathological conditions [8,9]. ZEB family contains ZEB1/ $\delta$ EF1 and ZEB2/SIP1. ZEB1 and ZEB2 could identify gene promoter on (CACCTG) sequence. ZEB2, also known as smad-interacting protein 1 (SIP1), plays an important role in normal physiogenesis. Researches show that ZEB2 overexpression increases the expression of matrix metalloproteinases (MMPs) family and aggravate endotheliocyte apoptosis [10]. Besides, ZEB2 has been reported to inhibit the apoptosis of tumor cells in bladder cancer [11].

Hyperglycemia could stimulate VECs to generate ROS and activate JNK pathway, which results in endotheliocyte apoptosis [12,13]. Our study aims to investigate the underlining regulatory mechanisms of ZEB2 on VECs apoptosis induced by high glucose and the correlative signal pathway.

## Material and Methods

### Cell culture

Human umbilical vein endothelial cells (HUVECs) were purchased from Shanghai Micro Mongolian Life Science Co., Ltd (Shanghai, China) and cultured in ECM medium (containing 5% fetal bovine serum, penicillin-streptomycin and  $1 \times$ EGFS, 37°C, 5%CO<sub>2</sub>, saturated humidity). When cells covered 80% culture bottle, HUVECs were passaged by 0.25% trypsin digestion. Then, HUVECs were added with ECM medium and centrifuged (1000rpm, 5minutes) to collect cells. With supernate

was abandoned, HUVECs were resuspended with ECM medium to adjust the density of  $5 \times 10^4$ /ml. Afterwards, HUVECs were seeded in culture plate with adherent culture.

### Transfection

ZEB2 upregulated and down-regulated plasmids (pEZ-M46-ES) were purchased from GeneCopoeia Company (Gene ID: NM\_014795). Cell transfection was performed with PEI (Polyscience, Cat#23966) transfection methods. Cells were seeded into six-well plates at a density of  $5 \times 10^4$  cells/wells to reach about 40–60% confluence for transfection. Plasmid and transfection reagents were blended (8  $\mu$ l siRNA duplexes and 6  $\mu$ l siRNA transfection reagent were added into 100  $\mu$ l siRNA transfection medium) and placed at room temperature for 15 min. the mixture was added with medium and cultured in incubator at 37°C, 5% CO<sub>2</sub> for 6 hours. After incubation, cells were replaced as conventional medium and cultured sequentially for 48 h.

### Grouping

Different groups of HUVECs were performed as experimental design. Normal group was treated with 5.5 mM glucose, and high-glucose groups were treated with 33 mM glucose. High-glucose groups were as follows: empty vector group (HUVECs), OE group (overexpression of ZEB2), LE group (lower-expression of ZEB2).

### Western blot

HUVECs were treated by RIPA Lysis Buffer System (Santa Cruz, Dallas, TX, USA). The liquid was transferred into sterile EP tube and centrifuged 12,000rpm for 10 minutes. Protein concentration was detected related to a known concentration of BCA. Two equal parts of proteins were mixed and sample buffers were subjected to SDS-PAGE. The separated protein was transferred onto PVDF membrane. Blocking buffer contained TBST and 5% fat-free milk. The PVDF membrane was blocked in blocking buffer for 1 hour at room temperature. Primary antibodies (Cell Signaling, 1: 1000) were diluted by 2% fat-free milk. The PVDF membrane was incubated with primary antibodies 4°C overnight and washed with TBST 3 times. Then, the PVDF membrane was diluted in secondary antibody (Santa Cruz, Dallas, USA, 1: 1000) 4°C overnight. Finally, the PVDF membrane was washed again with TBST 3 times for 10 minutes.  $\beta$ -actin acted as the internal reference. The PVDF membrane was displayed by Image Pro-Plus system (Media Cybernetics, Silver Spring, MD, USA).

### Real-time quantified PCR (RT-PCR)

The extracted RNA from HUVECs was treated with 1ml Trizol reagent (Invitrogen, Carlsbad, Calif, USA). The concentration

of RNA was detected at 260–280 nm and the qualified value was 1.8–2.0. The reverse transcription reaction system was 20  $\mu$ l (including 1  $\mu$ g RNA) to synthesize cDNA with SuperScript First-Strand Synthesis system (Invitrogen, Carlsbad, Calif, US). The reverse transcription reaction procedures were 42°C for 60 minutes for elongation and 95°C for 5 minutes for enzyme inactivation. Then, cDNA was synthesized and placed on ice for subsequent using. PCR amplification was carried out by ABI PRISM 7900 thermocycler (Applied Biosystems, US). The preliminary primers, synthesized by Sangon Biotech (Shanghai, China) were as follows: ZEB2, forward: 5'-GTGGA TGACC TAGGCA AGTCG-3', reverse: 5'-GTCTC CTCCT TGTTG TTCTGC-3'; GAPDH, forward, 5'-GCACC GTCAAGGCTGA GAAC-3', reverse 5'-TGGT GAAGACGCCAG TGG-3'. The reaction conditions were as follows: an initial denaturation step at 95°C for 4min; followed by 35 cycles at 94°C for 20s, 55°C for 30 seconds, 72°C for 20seconds, 72°C for 2 min, and a final elongation step at 72°C for 10 min. Relative levels of gene expression was expressed relative to  $\beta$ -actin and calculated using the  $2^{-\Delta\Delta Ct}$  method.

### MTT assay

The proliferation of HUVECs was detected by MTT Cell Proliferation and Cytotoxicity Assay Kit (Amyjet Scientific Inc., Wuhan, China). HUVECs were seeded in 96-well plates at the density of 8,000–10,000 cells per well with 200  $\mu$ l culture medium. Supernate was abandoned and then washed with PBS for 3 times. After 6, 12, 8 and 24 hours later, MTT (5 g/L, 20  $\mu$ l) solution was added to each well and the medium was incubated for another 4 h at 37°C. After centrifugation, supernatant was discarded and 200  $\mu$ l of DMSO was added to each well for dissolving the crystallization. The OD value was measured at 490 nm by a microplate reader (Tecan Sunrise, Mannedorf, Switzerland).

### Wound healing assay

HUVECs were seeded in 6-well plates and grew to about 90% confluence. With culture solution was discarded, the monolayer was wounded by manually scraping with a sterile pipette tip. After being washed with PBS for 3 times, HUVECs were added with fresh medium and incubated at 37°C. Images of wound closure were evaluated with an inverted microscope (Olympus, Japan) at sectionalized times. The migration rate was quantified with the distance between both sides of the edge. The migration rate was calculated by the formula: migration rate=migration distance/original distance.

### Measurement of reactive oxygen species (ROS) levels

Experiment operations were performed using the DCFDA-Cellular Reactive Oxygen Species Detection Assay Kit (Abcam, ab113851) according to the manufacturer instructions. Briefly,

DCFH-DA was diluted by serum-free culture medium to final concentration of 10  $\mu$ mol/l. After being digested by trypsin from culture plate and centrifuged (10,000g), HUVECs were resuspended in the 10  $\mu$ mol/l DCFH-DA at a density  $1 \times 10^6$  cells/ml. Then, HUVECs were incubated in incubator at 37°C in the dark for 20 min, and then washed with serum-free for 3 times to clear the residual DCFH-DA. Fluorescence intensity was measured for DCF fluorescence with a flow cytometer (Becton, Dickinson and Company, New York, USA) and results were corrected for cell number according to the manufacturer instructions at 530 nm. In addition to those mentioned above, conditions used include hypoxanthine as a positive control and leads to a maximum fluorescent signal in both control and CDH PAEC.

### Flow cytometry

Apoptotic cells were identified by Annexin V-FITC/PI double staining with Dead Cell Apoptosis Kit (Invitrogen USA). Briefly, cells were seeded in 6-well plates ( $4 \times 10^5$  per well). HUVECs were harvested and digested by pancreatin without EDTA. After being washed with PBS for 2 times, HUVECs were resuspended in Annexin-binding buffer, and 5  $\mu$ l Annexin V-FITC and 5  $\mu$ l PI were added before incubating at room temperature for 10–15 mins in dark. FITC and PI fluorescence were analyzed by flow cytometry.

### Statistical analysis

The results were presented as means  $\pm$ SEM. All data were recorded and analyzed with SPSS 17.0 software (Chicago, IL, USA). The differences between individual groups were analyzed by one-way ANOVA followed by Fisher's LSD test.  $P < 0.05$  was considered statistically significant.

## Results

### Upregulated and down-regulated expression of ZEB2

In order to validate the function of ZEB2 on HUVECs, upregulated and down-regulated expressions of ZEB2 were performed by plasmid transfection (Figure 1). HUVECs were respectively treated with different concentrations of glucose (5.5 mM, 33 mM). then, protein and mRNA expression levels of ZEB2 were detected by western blot and RT-qPCR. Protein expressions of ZEB2 in upregulated (overexpression, OE) and down-regulated (lower-expression, LE) group were statistically higher or lower than that in normal glucose (5.5 mM) group. These results indicated that plasmid transfection successfully established the ZEB2 overexpression and underexpression cells model.

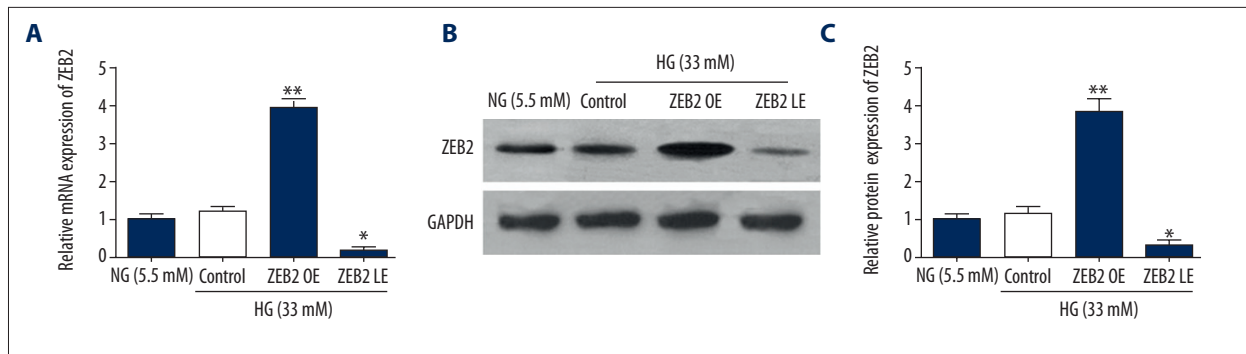


**Figure 1.** ZEB2 expression in HUVECs mediated by plasmids transfection. **(A)** The expression of ZEB2 mRNA was detected by RT-qPCR. **(B)** The expression of ZEB2 protein was analyzed by western blot. Data represent means  $\pm$  standard deviation. \*  $P < 0.05$ , \*\*  $P < 0.01$  compared with empty vector group. OE and LE groups respectively represents overexpression and lower-expression of ZEB2. NG represents normal glucose, and HG represents high glucose.

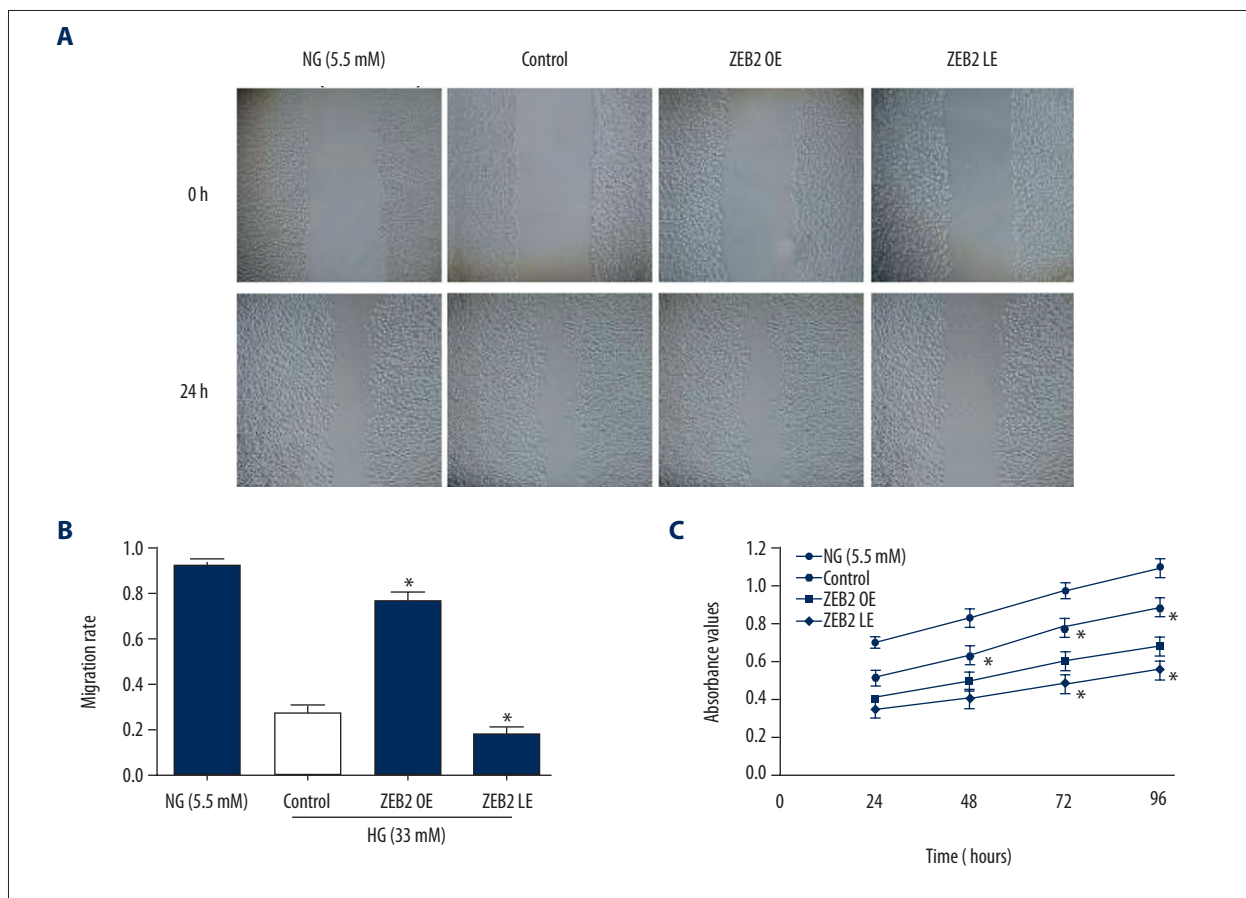


**Figure 2.** Migration and proliferation vitality of HUVECs were detected by wound healing and MTT assay. **(A)** Wound healing was performed at time-points 0 and 24 hours. **(B)** Migration rate of HUVECs in each group. **(C)** Proliferation vitality was respectively detected by MTT at 24, 48, 72, and 96 hours. Experiments data were performed in triplicate. \*  $P < 0.05$  compared with the control group.

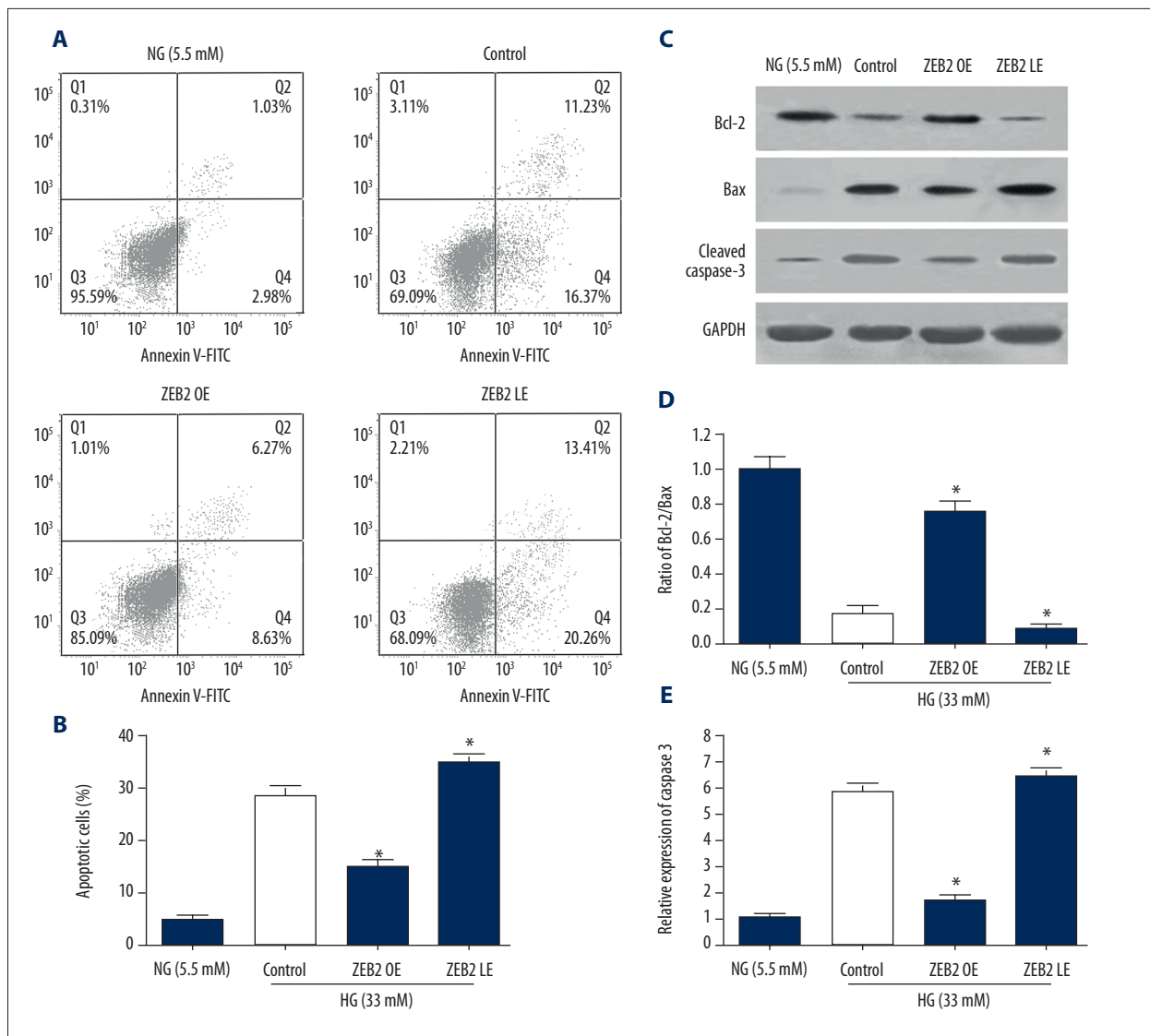


**Figure 3.** Apoptosis of HUVECs induced by high glucose was detected by flow cytometry and western blot. **(A)** HUVECs were stained with Annexin V-FITC/PI for flow cytometry analysis. Apoptotic cells were divided into 2 stages (early apoptotic, late apoptotic cells). **(B)** The total apoptotic rates examined by flow cytometry, including the early and late apoptosis rate. **(C)** Representative bands of Bcl-2, Bax and caspase 3 detected by western blot. **(D)** Ratio of Bcl-2/Bax. **(E)** Ratio of cleaved caspase 3. Data represent means  $\pm$  standard deviation. \*  $P < 0.05$  compared with control group.

### HUVECs proliferation and migration

Proliferation and migration of HUVECs were detected by MTT assay and wound healing (Figure 2). In the high glucose environment (33 mM), proliferative and migration activity of HUVECs were obviously inhibited compared with normal glucose concentration (5.5 mM). Nevertheless, ZEB2 overexpression rescued the proliferative and migration activity of HUVECs. However, ZEB2 underexpression mildly inhibited the proliferative and migration activity. These results showed that ZEB2 overexpression could alleviate the inhibitory state induced by hyperglycemia.

### Apoptosis of HUVECs induced by high glucose

To examine the role of ZEB2 on the regulation of endothelium, the apoptosis of HUVECs induced by high glucose was detected by flow cytometry and western blot (Figure 3). As shown in Figure 3A and 3B, FCM showed that the percentage of apoptotic HUVECs was elevated observably in high glucose group compared to NG (5.5 mM) group, indicating that high glucose (33 mM) promoted the apoptosis of HUVECs. Then, with ZEB2 expression being upregulated, the apoptosis of HUVECs was inhibited effectively, indicating that ZEB2 could protect HUVECs from apoptosis. However, the apoptosis of



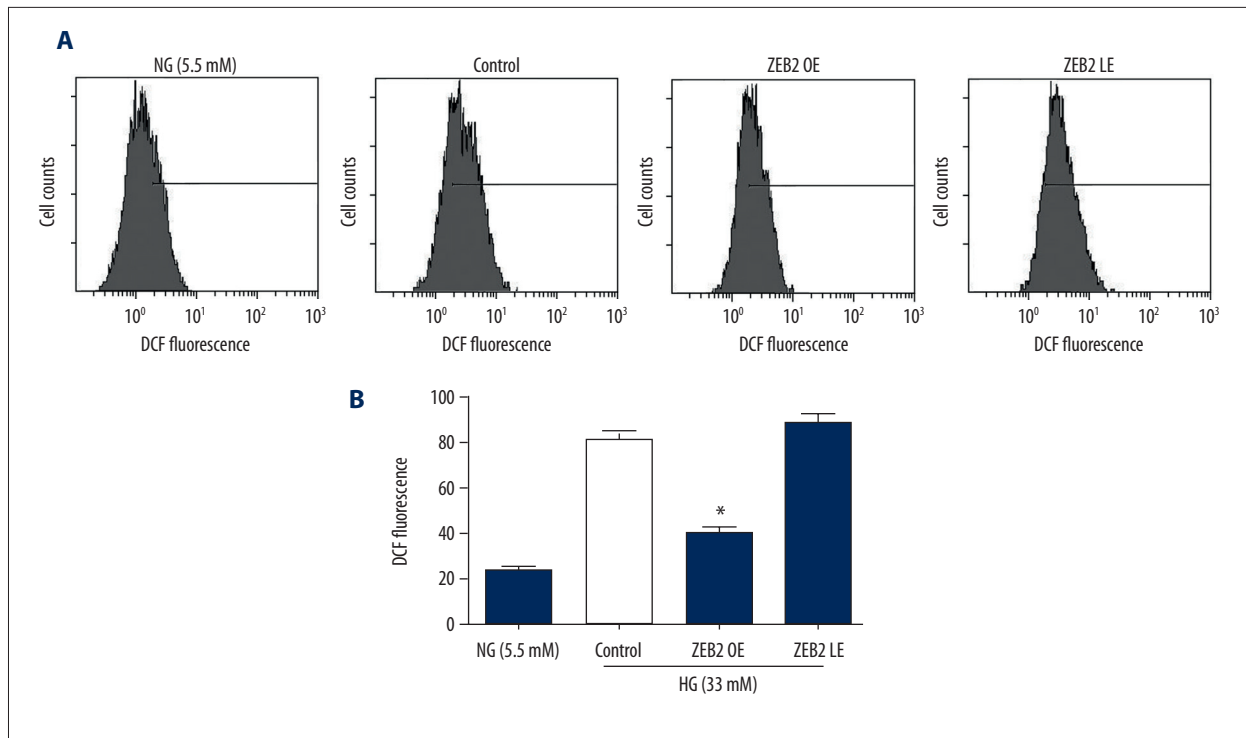


**Figure 4.** The levels of intracellular ROS were detected by flow cytometry. (A) ROS in HUVECs that were treated with different concentrations of glucose (5.5 mM, 33 mM) was analyzed after 24 h by flow cytometry. (B) Data of ROS expression were expressed as mean  $\pm$ SD of 4 independent groups. The superscript letter on columns represented that \*  $P < 0.05$  compared with control group.

HUVECs was mildly aggravated in ZEB2 down-regulated group (LE group). Correspondingly, as shown in Figure 3C–3E, Western blot showed that Bcl-2, Bax and cleaved caspase 3 revealed the similar condition with flow cytometry. In high glucose control group, the Bcl-2/Bax ratio was decreased and cleaved caspase 3 was increased, suggesting that high glucose facilitated the apoptosis of HUVECs. Afterwards, ZEB2 overexpression increased the Bcl-2/Bax ratio and decreased cleaved caspase 3, while ZEB2 underexpression mildly decreased Bcl-2/Bax ratio and increased cleaved caspase 3. Above results demonstrated that ZEB2 overexpression distinctly suppressed the apoptosis of HUVECs induced by high glucose.

#### Measurement of intracellular reactive oxygen species (ROS) levels

The levels of intracellular ROS in 4 experimental groups were detected by flow cytometry (Figure 4). HUVECs were treated with different concentrations of glucose (5.5 mM, 33 mM). ROS expression was upregulated in high glucose group compared to normal glucose group. Besides, overexpression of ZEB2 observably decreased the ROS expression, while lower-expression of ZEB2 slightly enhanced the expression of ROS. The results showed that ZEB2 could suppress the expression of ROS, which might be an approach of apoptosis inhibition by ZEB2.

#### ZEB2 regulated the MAPK pathway

The regulation of ZEB2 on MAPK pathway was detected by western blot (Figure 5). In high glucose (33 mM) culture medium, phosphorylation of p38, JNK and ERK1/2 were statistically increased in HUVECs compared with normal glucose (5.5 mM). Afterwards, phosphorylation of JNK was obviously suppressed by ZEB2 overexpression in OE group, which was mildly increased by ZEB2 lower-expression in LE group. However, p38 and ERK were not obviously affected by up- or down-regulation of ZEB2. Above results showed that high glucose activates MAPK pathway, and ZEB2 overexpression could repress the phosphorylation of JNK pathway.

#### Discussion

ZEB2, one of the important members of the ZEB transcription factors family, recognizes and combines the E2 boxes of target gene promoter region to regulate gene expression. ZEB2 has been reported to participate in the regulation of epithelial-mesenchymal transition. Our study aims to investigate the regulation of ZEB2 on the apoptosis and proliferation of vascular endothelial cells (VECs) through MAPK pathway.

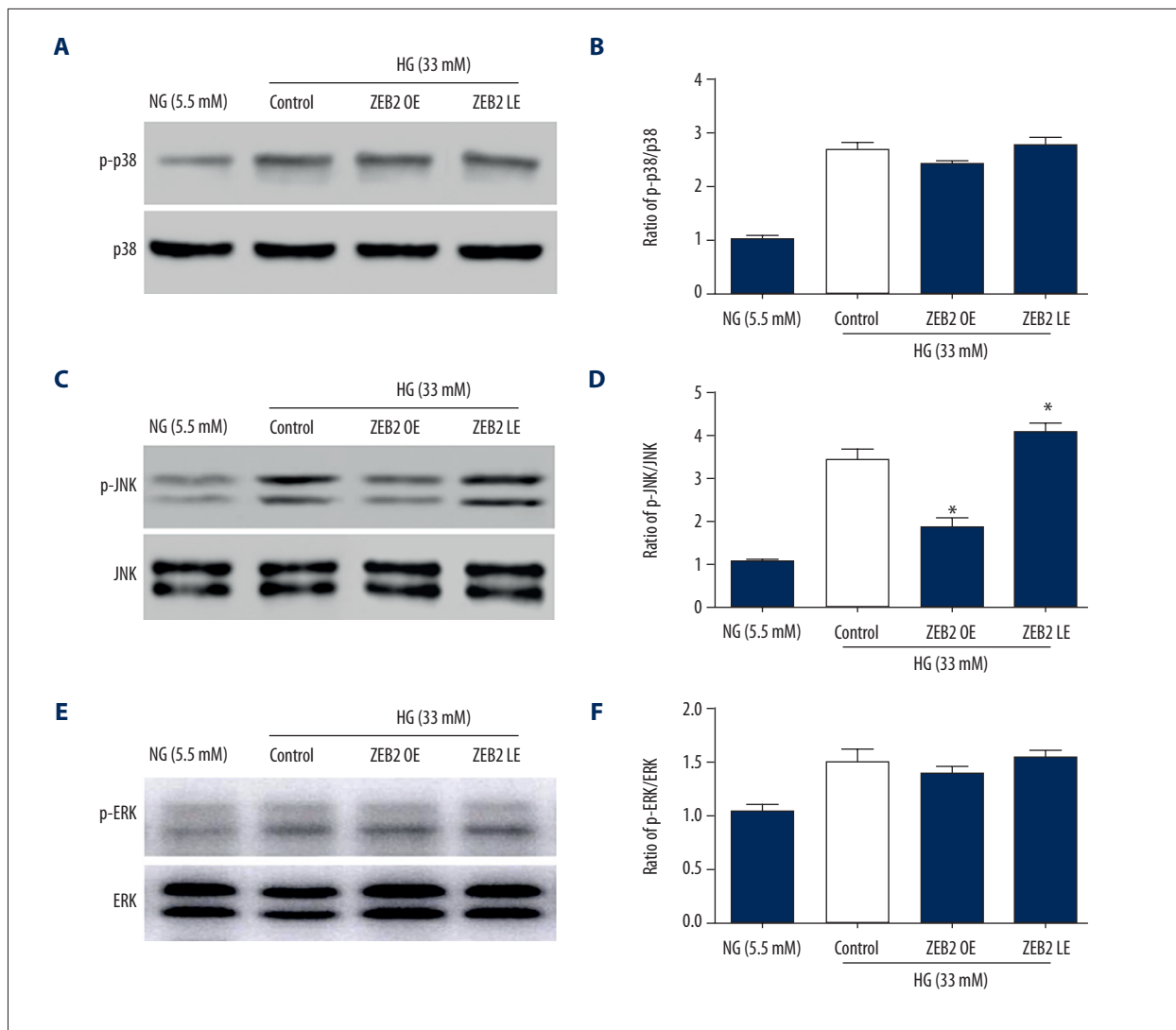


**Figure 5.** Phosphorylation activities of p38, JNK, ERK1/2 were detected by western blot. (**A, C, E**) Typical bands of p38, JNK, ERK in NG group (5.5 mM) and HG group (33 mM). (**B, D, F**) Relative quantified expression p-p38/p38, p-JNK/JNK, p-ERK/ERK. \*  $P < 0.05$  compared with the control group.

Our study chooses HUVECs to be the experimental cells. On this basis, plasmid transfection was performed to establish ZEB2 upregulated and down-regulated models. HUVECs are respectively treated with different concentrations of glucose (5.5 mM, 33 mM). Western blot and RT-qPCR show that protein and mRNA expression of ZEB2 were statistically upregulated and down-regulated through plasmid transfection (Figure 1). After plasmid transfection, ZEB2 overexpression promotes the proliferative and migration activity of HUVECs (Figure 2).

ZEB2 not only participates in the regulation of epithelial-mesenchymal transition, but also resists tumor cell apoptosis and regulate cell cycle. The apoptosis of HUVECs detected by flow cytometry and western blot reveals that ZEB2 overexpression distinctly suppressed the apoptosis of HUVECs induced by high

glucose (Figure 3). Presently, some mechanisms could illuminate the pathogenesis of vascular complications induced by high glucose [14]. Among them, certain approaches are activated by hyperglycemia and act reciprocally. The most likely reason for the activation might be the massive generation of ROS induced by hyperglycemia [15]. Another study also finds ZEB2 play a significant role of anti-oncogene and its overexpression could induce the phosphorylation of retinoblastoma tumor-suppressor protein to impede cell cycle G1 phase through inhibiting cyclin D1 transcription [16]. From the study of bladder cancer, ZEB2 play a role of anti-apoptosis and involve in progress of the bladder cancer, induced by no matter cisplatin or ultraviolet ray [17]. Furthermore, ZEB2 could negative regulative human telomerase reverse transcriptase through TGF- $\beta$  dependent pattern to promote the aging of

cancer cell [18]. ROS could mediate growth, proliferation and apoptosis of VECs, and it's also able to adjust the diastolic and retractile function of blood vessels [19]. In our study, ZEB2 suppresses the expression of ROS (Figure 4), which might be an approach of apoptosis inhibition by ZEB2. Upregulated expression of ROS in HUVECs indicates that high glucose could enhance oxidative stress response to cause endothelial injury [20,21]. Overexpression of ZEB2 decreases the synthesis of ROS induced by hyperglycemia to reduce the oxidative stress response. The possible mechanism might be illuminated that ZEB2 suppresses the expression and activity of Rac1 gene and reduce the generation of active oxygen clusters, such as H<sub>2</sub>O<sub>2</sub>, to inhibit intracellular oxidation [22,23].

In HUVECs, high glucose activates the MAPK pathway. The phosphorylation level of p38, JNK, and ERK are increased in high concentration of glucose (33 mM). Our study finds that ZEB2 overexpression could enhance the phosphorylation level of JNK pathway (Figure 5). However, the phosphorylation levels of p38 and ERK are stable without variation in up- or down-regulated groups. Research has confirmed that high glucose

could sequentially activate JNK and cysteine protease-3 (caspase-3) through oxidative stress; however, JNK1 antisense oligonucleotide can inhibit the activity of caspase 3 and block apoptosis [24]. In patients with type 2 diabetes and in diabetic animal models, it has been found that JNK activity is significantly increased [25]. In a high glucose environment, the JNK pathway can also regulate cell apoptosis process through transcription activity of NF-κB [26].

## Conclusions

Generally, above results could partly explain the mechanism of vascular lesions induced by high glucose and provides a novel insight and therapeutic target for diabetic vascular disease and its complications.

## Acknowledgement

The authors want to thank Dr. Lu for her technical help and manuscript correcting.

## Reference:

1. Wang F, Jia J, Lal N et al: High glucose facilitated endothelial heparanase transfer to the cardiomyocyte modifies its cell death signature. *Cardiovas Res*, 2016; 112: 656–68
2. Chu P, Han G, Ahsan A et al: Phosphocreatine protects endothelial cells from Methylglyoxal induced oxidative stress and apoptosis via the regulation of PI3K/Akt/eNOS and NF-kappaB pathway. *Vascul Pharmacol*, 2016 [Epub ahead of print]
3. Cai W, Torreggiani M, Zhu L et al: AGER1 regulates endothelial cell NADPH oxidase-dependent oxidant stress via PKC-delta: Implications for vascular disease. *American journal of physiology Cell Physiol*, 2010; 298: C624–34
4. Carlomosti F, D'Agostino M, Beji S et al: Oxidative stress-induced miR-200c disrupts the regulatory loop among SIRT1, FOXO1 and eNOS. *Antioxid Redox Signal*, 2016 [Epub ahead of print]
5. Sun X, Jiao X, Ma Y et al: Trimethylamine N-oxide induces inflammation and endothelial dysfunction in human umbilical vein endothelial cells via activating ROS-TXNIP-NLRP3 inflammasome. *Biochem Biophys Res Commun*, 2016; 481: 63–70
6. Ashor AW, Chowdhury S, Oggioni C et al: Inorganic nitrate supplementation in young and old obese adults does not affect acute glucose and insulin responses but lowers oxidative stress. *J Nutr*, 2016; 146: 2224–32
7. Kuate D, Kengne AP, Biapa CP et al: Tetrapleura tetraptera spice attenuates high-carbohydrate, high-fat diet-induced obese and type 2 diabetic rats with metabolic syndrome features. *Lipids Health Dis*, 2015; 14: 50
8. Clarhaut J, Gemmill RM, Potiron VA et al: ZEB-1, a repressor of the semaphorin 3F tumor suppressor gene in lung cancer cells. *Neoplasia (New York, NY)*, 2009; 11: 157–66
9. Nishijima N, Seike M, Soeno C et al: miR-200/ZEB axis regulates sensitivity to nintedanib in non-small cell lung cancer cells. *Int J Oncol*, 2016; 48: 937–44
10. Li SH, Fu J, Watkins DN et al: Sulforaphane regulates self-renewal of pancreatic cancer stem cells through the modulation of Sonic hedgehog-Gli pathway. *Mol Cell Biochem*, 2013; 373: 217–27
11. Sayan AE, Griffiths TR, Pal R et al: SIP1 protein protects cells from DNA damage-induced apoptosis and has independent prognostic value in bladder cancer. *Proc Natl Acad Sci USA*, 2009; 106: 14884–89
12. Kaneto H, Matsuoka TA, Nakatani Y et al: Oxidative stress and the JNK pathway in diabetes. *Curr Diabetes Rev*, 2005; 1: 65–72
13. Yarza R, Vela S, Solas M, Ramirez MJ: c-Jun N-terminal kinase (JNK) signaling as a therapeutic target for Alzheimer's disease. *Front Pharmacol*, 2015; 6: 321
14. Qin W, Ren B, Wang S et al: Apigenin and naringenin ameliorate PKCbeta1-associated endothelial dysfunction via regulating ROS/caspase-3 and NO pathway in endothelial cells exposed to high glucose. *Vascul Pharmacol*, 2016; 85: 39–49
15. Eleftheriadis T, Tsogka K, Pissas G et al: Activation of general control non-repressible 2 kinase protects human glomerular endothelial cells from harmful high-glucose-induced molecular pathways. *Int Urol Nephrol*, 2016; 48: 1731–39
16. Egger JV, Lane MV, Antonucci LA et al: Dephosphorylation of the Retinoblastoma protein (Rb) inhibits cancer cell EMT via Zeb. *Cancer Biol Ther*, 2016; 17: 1197–205
17. Yun SJ, Kim WJ: Role of the epithelial-mesenchymal transition in bladder cancer: From prognosis to therapeutic target. *Korean J Urol*, 2013; 54: 645–50
18. Tange S, Oktyabri D, Terashima M et al: JARID2 is involved in transforming growth factor-beta-induced epithelial-mesenchymal transition of lung and colon cancer cell lines. *PLoS One*, 2014; 9: e115684
19. Paulus WJ, Tschope C: A novel paradigm for heart failure with preserved ejection fraction: comorbidities drive myocardial dysfunction and remodeling through coronary microvascular endothelial inflammation. *J Am Coll Cardiol*, 2013; 62: 263–71
20. Alinovi R, Goldoni M, Pinelli S et al: Oxidative and pro-inflammatory effects of cobalt and titanium oxide nanoparticles on aortic and venous endothelial cells. *Toxicology In Vitro*, 2015; 29: 426–37
21. Costa TJ, Ceravolo GS, dos Santos RA et al: Association of testosterone with estrogen abolishes the beneficial effects of estrogen treatment by increasing ROS generation in aorta endothelial cells. *Am J Physiol Heart Circ Physiol*, 2015; 308(7): H723–32
22. Cheng PW, Lee HC, Lu PJ et al: Resveratrol inhibition of Rac1-derived reactive oxygen species by AMPK decreases blood pressure in a fructose-induced rat model of hypertension. *Sci Rep*, 2016; 6: 25342
23. Holzner S, Senfter D, Stadler S et al: Colorectal cancer cell-derived microRNA200 modulates the resistance of adjacent blood endothelial barriers *in vitro*. *Oncol Rep*, 2016; 36: 3065–71



24. Ho FM, Lin WW, Chen BC et al: High glucose-induced apoptosis in human vascular endothelial cells is mediated through NF-kappaB and c-Jun NH2-terminal kinase pathway and prevented by PI3K/Akt/eNOS pathway. *Cell Signal*, 2006; 18: 391–99
25. Kim SW, Kim CE, Kim MH: Flavonoids inhibit high glucose-induced up-regulation of ICAM-1 via the p38 MAPK pathway in human vein endothelial cells. *Biochem Biophys Res Commun*, 2011; 415: 602–7
26. Guan G, Han H, Yang Y et al: Neferine prevented hyperglycemia-induced endothelial cell apoptosis through suppressing ROS/Akt/NF-kappaB signal. *Endocrine*, 2014; 47: 764–71